

Supporting Information

Dissymmetry Factor Spectral Analysis Can Provide Useful Diastereomer Discrimination: Chiral Molecular Structure of an Analogue of (-)-Crispine A

Jordan L. Johnson[‡], Divya Sadasivan Nair[†], Sarath Muraleedharan Pillai[†], Didimos Johnson[†], Zabeera Kallingathodi[†], Ibrahim Ibnusaud^{†*} and Prasad L. Polavarapu^{‡*}

[‡]Department of Chemistry, Vanderbilt University, Nashville, TN 37235 USA

[†]Institute for Intensive Research in Basic Sciences, Mahatma Gandhi University, P.D. Hills P.O., Kottayam, Kerala 686560, India

Table S1. Crystal data and structure refinement for 5

Empirical formula	C ₁₆ H ₂₃ NO ₇
Formula weight	341.35
Temperature	296(2) K
Wavelength	0.71073 Å
Crystal system	Orthorhombic
Space group	P 21 21 21
Unit cell dimensions	a = 5.674(3) Å; α= 90°. b = 10.990(7) Å; β= 90°. c = 26.414(16) Å; γ = 90°.
Volume	1647.2(17) Å ³
Z	4
Density (calculated)	1.376 Mg/m ³
Absorption coefficient	0.108 mm ⁻¹
F(000)	728
Crystal size	0.800 x 0.600 x 0.400 mm ³
Theta range for data collection	3.085 to 19.732°.
Index ranges	-5<=h<=5, -10<=k<=10, -24<=l<=24
Reflections collected	7946
Independent reflections	1466 [R(int) = 0.2462]
Completeness to theta = 19.732°	98.60%
Refinement method	Full-matrix least-squares on F ²
Data / restraints / parameters	1466 / 0 / 226
Goodness-of-fit on F2	1.027
Final R indices [I>2sigma(I)]	R1 = 0.0832, wR2 = 0.1605
R indices (all data)	R1 = 0.1702, wR2 = 0.1998
Absolute structure parameter	-5.8(10)
Extinction coefficient	0.033(8)
Largest diff. peak and hole	0.266 and -0.257 e.Å ⁻³

Table S2. Bond lengths [\AA] and angles [$^\circ$] in crystal structure of **5**

O(3)-C(12)	1.256	C(6)-C(7)-C(8)	120.6
O(4)-C(14)	1.403	C(6)-C(7)-C(11)	121.9
O(5)-C(15)	1.422	C(8)-C(7)-C(11)	117.2
O(1)-C(4)	1.374	C(14)-C(13)-C(12)	103.2
O(1)-C(1)	1.397	N(1)-C(11)-C(7)	110.5
N(1)-C(12)	1.31	N(1)-C(11)-C(14)	102.4
N(1)-C(11)	1.452	C(7)-C(11)-C(14)	118
N(1)-C(10)	1.457	C(5)-C(4)-C(3)	121
O(2)-C(3)	1.34	C(5)-C(4)-O(1)	123
O(2)-C(2)	1.42	C(3)-C(4)-O(1)	115.8
C(7)-C(6)	1.381	O(4)-C(14)-C(13)	111.5
C(7)-C(8)	1.39	O(4)-C(14)-C(15)	108.6
C(7)-C(11)	1.53	C(13)-C(14)-C(15)	114.7
C(13)-C(14)	1.5	O(4)-C(14)-C(11)	105.7
O(6)-C(16)	1.422	C(13)-C(14)-C(11)	99.4
C(13)-C(12)	1.52	C(15)-C(14)-C(11)	116.4
C(11)-C(14)	1.559	O(5)-C(15)-C(16)	109
C(4)-C(5)	1.36	O(5)-C(15)-C(14)	106.3
C(4)-C(3)	1.36	C(16)-C(15)-C(14)	116.5
C(14)-C(15)	1.5	C(7)-C(6)-C(5)	116.7
C(15)-C(16)	1.46	C(7)-C(6)-C(9)	119.6
C(6)-C(5)	1.42	C(5)-C(6)-C(9)	123.7
C(6)-C(9)	1.5	C(9)-C(10)-N(1)	107.1
C(10)-C(9)	1.46	O(3)-C(12)-N(1)	126.3
C(3)-C(8)	1.38	O(3)-C(12)-C(13)	125.2
C(4)-O(1)-C(1)	117.2	N(1)-C(12)-C(13)	108.5
C(12)-N(1)-C(11)	111.9	O(2)-C(3)-C(4)	116
C(12)-N(1)-C(10)	125	O(2)-C(3)-C(8)	125
C(11)-N(1)-C(10)	123	C(4)-C(3)-C(8)	118.8
C(3)-O(2)-C(2)	115.7	C(3)-C(8)-C(7)	121.1

Table S3: VCD Band assignments for (*1R,10bR,1'R*) diastereomer

In the B3PW91/6-311++G(2d,2p)/PCM(methanol) predicted VCD spectrum, the VCD band positions and the associated vibrational modes are as follows:

1713 cm⁻¹ negative band: carbonyl stretching

1548 cm⁻¹ negative band: in-plane C-H bending of the benzene ring

1491 cm⁻¹ positive band: CH₂ bending at C5

1472 cm⁻¹ negative band: CH₂ bending at C5 and C6; and CH₃ bending of methoxy groups

1429 cm⁻¹ negative band: CH₃ bending of both methoxy groups, CH₂ bending at C2 and C-C stretching of the benzene ring

1323 cm⁻¹ negative band: CH₂ bend at C5, C6 and CH bend at C1'

1287 cm⁻¹ negative band: in-plane C-H bending of benzene ring and C-H bending at C10b

1247 cm⁻¹ positive band: predominantly from CH₂ bend at C6.

1231 cm⁻¹ negative band: CH₂ bending at C6 and C-H bend of benzene

Table S4: Energies, Populations^a, and Ring Puckering Angles for Conformers of Three Diastereomers with Deuterated OH Groups at B3PW91/6-311++G(2d,2p)/PCM (Methanol)

Conformer	Gibbs Energy	Energy (kcal/mol)	Population	N4-C5-C6-C6a	C1-C2-C3-N4
(1 <i>R</i> ,10 <i>bS</i> ,1' <i>R</i>)					
20	-1128.07	0.00	0.42	48.3	15.1
140	-1128.07	0.15	0.33	51.8	21.0
150	-1128.07	0.44	0.20	51.9	19.6
483	-1128.07	1.51	0.03	47.9	20.9
119	-1128.07	2.49	0.01	51.9	19.7
(1 <i>S</i> ,10 <i>bR</i> ,1' <i>R</i>)					
113	-1128.07	0.00	0.52	-49.2	-14.7
28	-1128.07	1.19	0.07	-52.5	-20.7
85	-1128.07	1.23	0.06	-49.5	-16.8
10	-1128.07	1.30	0.06	-52.1	-20.0
142	-1128.07	1.32	0.05	-52.4	-21.1
178	-1128.07	1.32	0.05	-52.4	-21.0
561	-1128.07	1.50	0.04	-50.8	-17.0
383	-1128.07	1.55	0.04	-50.7	-16.9
185	-1128.07	1.69	0.03	-49.1	-14.3
81	-1128.07	1.77	0.03	-52.7	-20.7
77	-1128.07	1.89	0.02	-49.2	-15.2
74	-1128.07	1.96	0.02	-49.3	-14.9
12	-1128.06	2.63	0.01	-52.7	-20.6
(1 <i>S</i> ,10 <i>bS</i> ,1' <i>R</i>)					
33	-1128.07	0.00	0.74	52.5	20.5
86	-1128.07	1.19	0.10	53.0	21.4
50	-1128.07	1.50	0.06	51.4	18.4
11	-1128.07	1.73	0.04	52.6	20.3
44	-1128.07	1.80	0.03	52.6	20.3
60	-1128.07	1.93	0.03	49.6	15.6
177	-1128.07	2.91	0.01	52.8	19.5

^aOnly conformers with population of at least 1% are listed

Table S5: SSO values^a of VDF spectra with maximum magnitudes for OH deuterated diastereomers as a function of experimental reliability criterion

Diastereomer	<i>SimVDF</i>		
	0 ppm	10 ppm	40 ppm
(1 <i>R</i> ,10b <i>R</i> ,1' <i>R</i>)	0.65	0.66	0.61
(1 <i>R</i> ,10b <i>S</i> ,1' <i>R</i>)	-0.37	-0.35	-0.23
(1 <i>S</i> ,10b <i>R</i> ,1' <i>R</i>)	0.35	0.36	0.16
(1 <i>S</i> ,10b <i>S</i> ,1' <i>R</i>)	-0.45	-0.46	-0.44

^a1160–1800 cm⁻¹ region used for VCD and VDF similarity overlap analyses

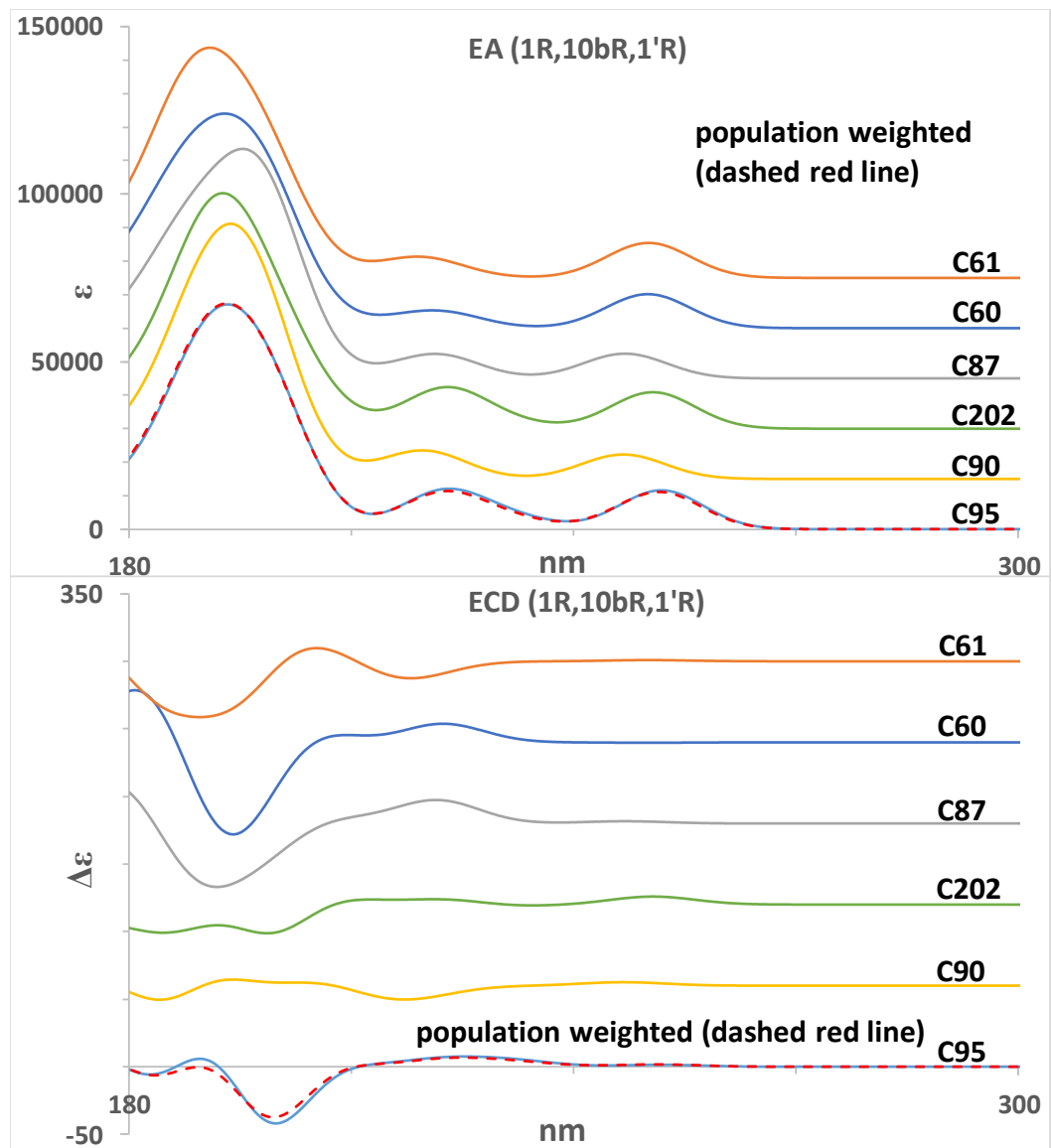


Figure S1: EA and ECD spectra for individual conformers of (1*R*,10*bR*,1'*R*) diastereomer and population weighted spectra.

Transition at 252 nm ECD

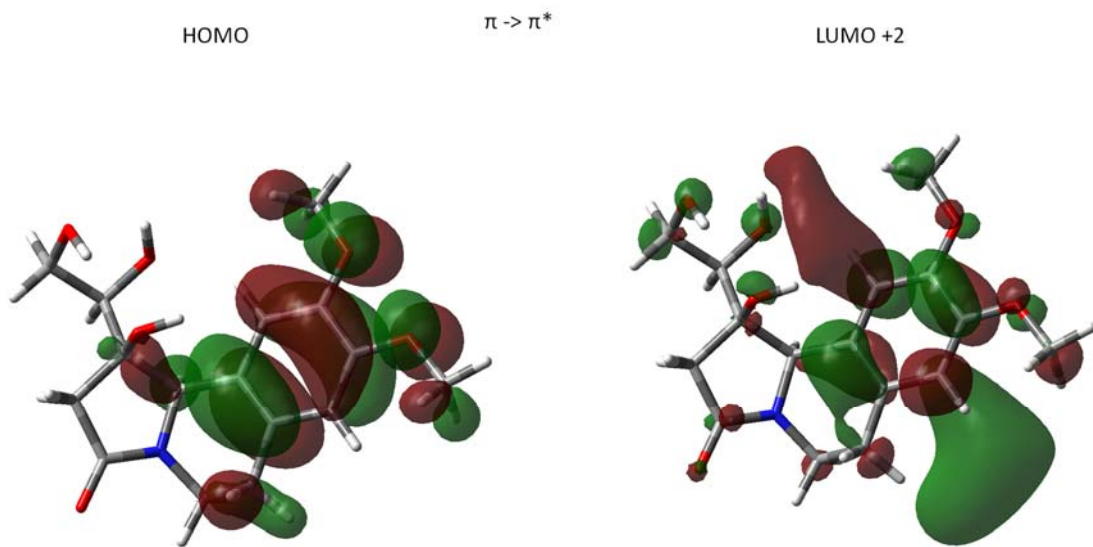


Figure S2. MOs responsible for the 252 nm transition.

Transition at 226 nm in ECD

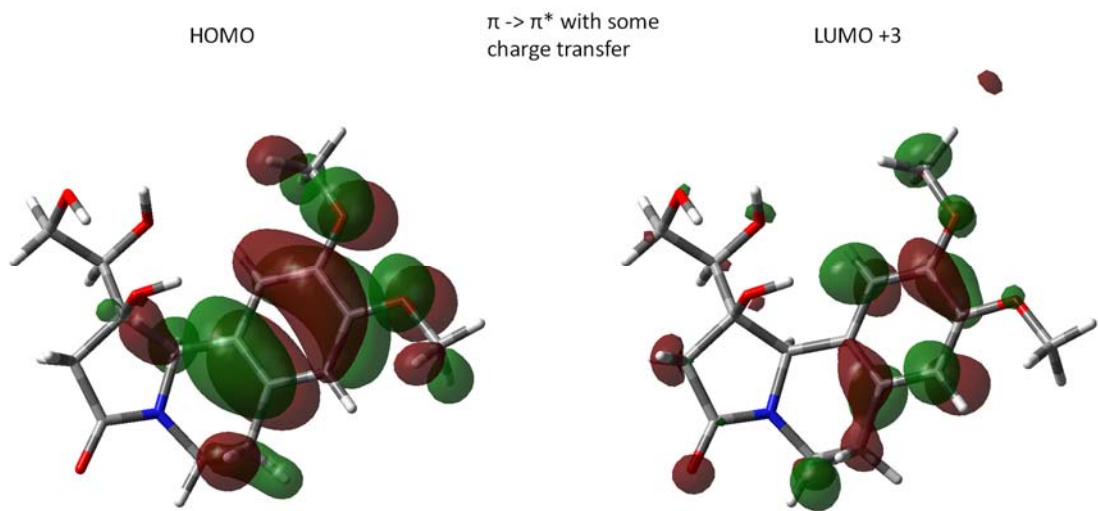


Figure S3. MOs responsible for the 226 nm transition.

Transition at 200 nm in ECD

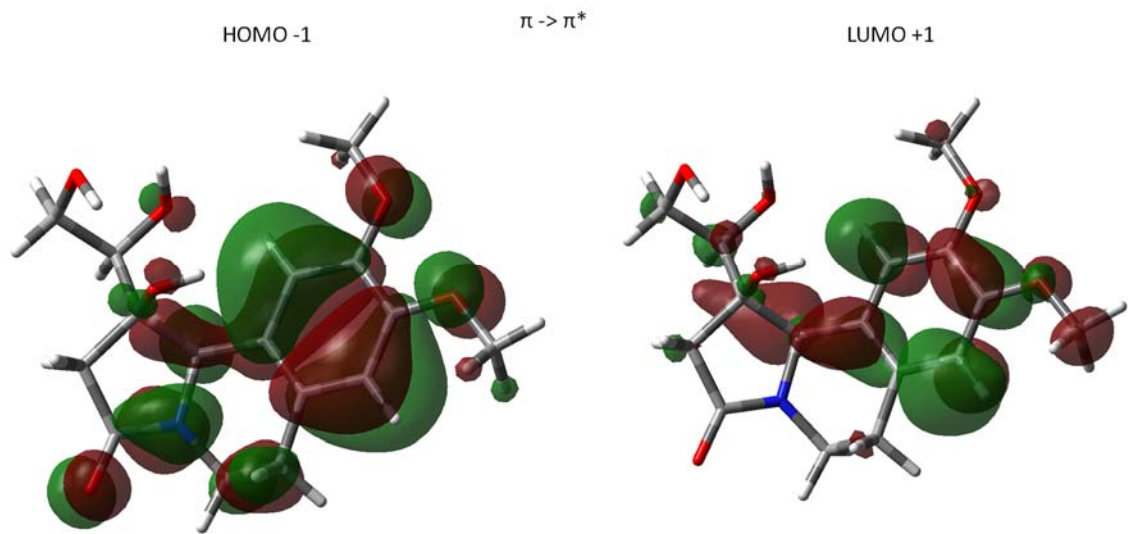


Figure S4. MOs responsible for the 200 nm transition.

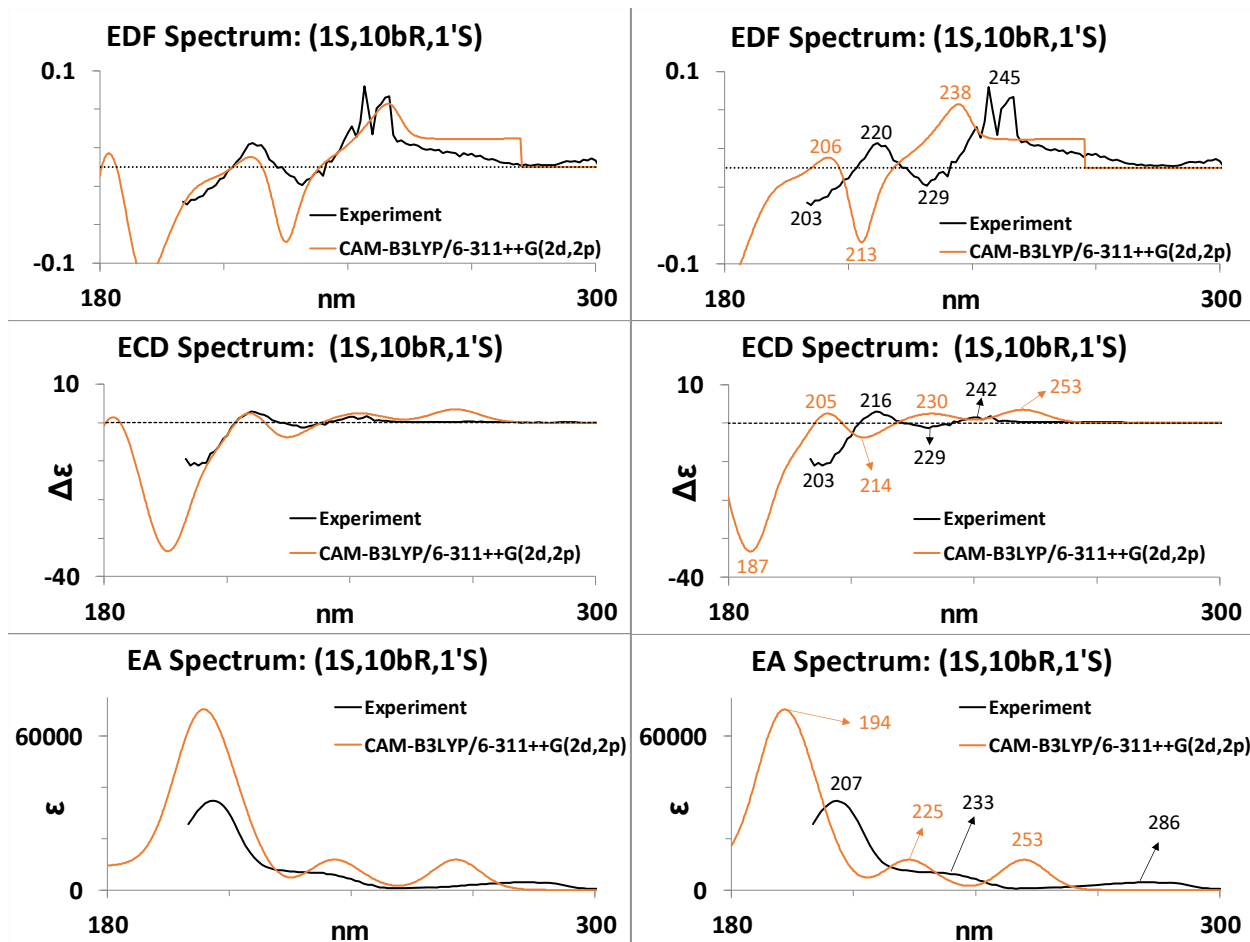


Figure S5. Comparison of experimental EA, ECD and EDF spectra of **5** with those predicted for (*1S,10bR,1'S*) diastereomer. The ECD spectra for (*1S,10bR,1'S*) diastereomer were obtained by multiplying the ECD of (*1R,10bS,1'R*) diastereomer with -1. In the left vertical panel, the predicted wavelengths are scaled with 1.055 (which corresponds to maximum *SimECD* value) and overlaid on experimental spectra. In the right vertical panel, QC predicted spectra obtained with unscaled band positions are presented.

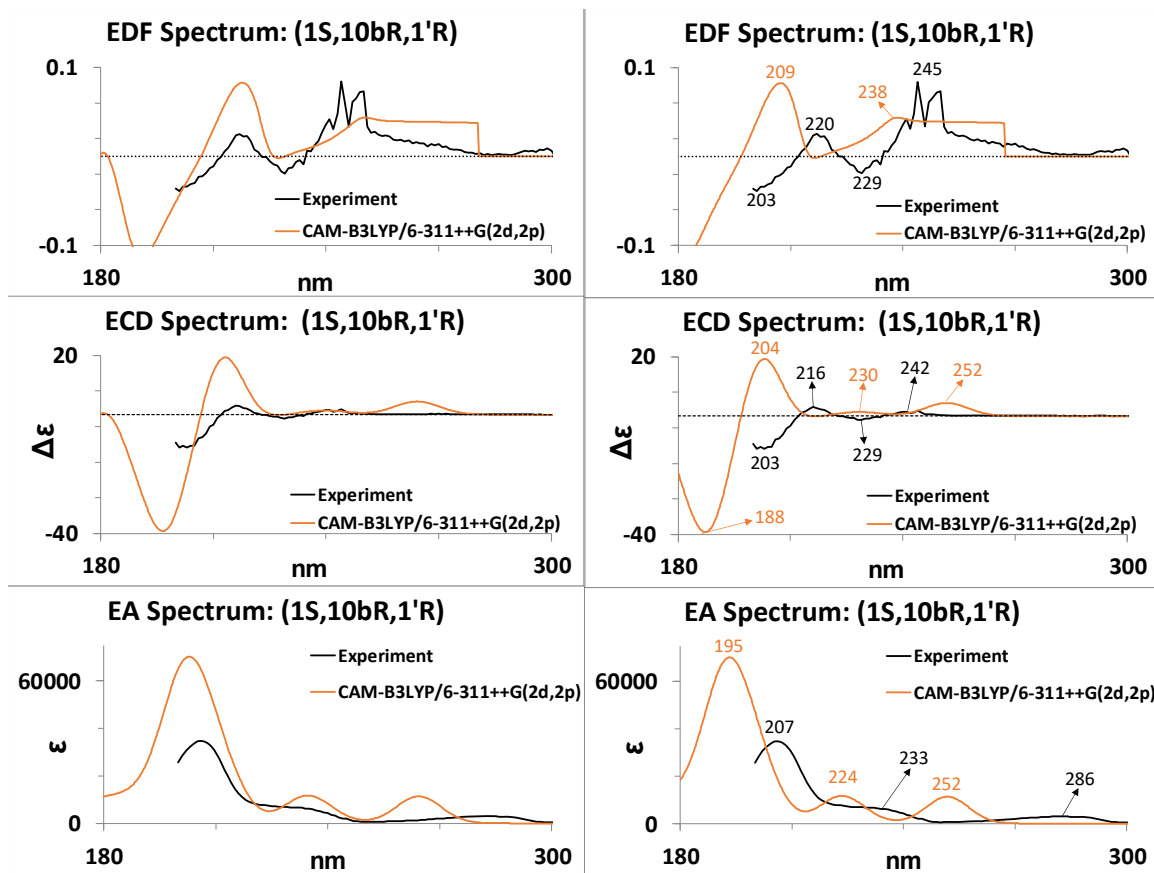


Figure S6. Comparison of experimental EA, ECD and EDF spectra of **5** with those predicted for (1S,10bR,1'R) diastereomer. In the left vertical panel, the predicted wavelengths are scaled with 1.05 (which corresponds to maximum *SimECD* value) and overlaid on experimental spectra. In the right vertical panel, QC predicted spectra obtained with unscaled band positions are presented.

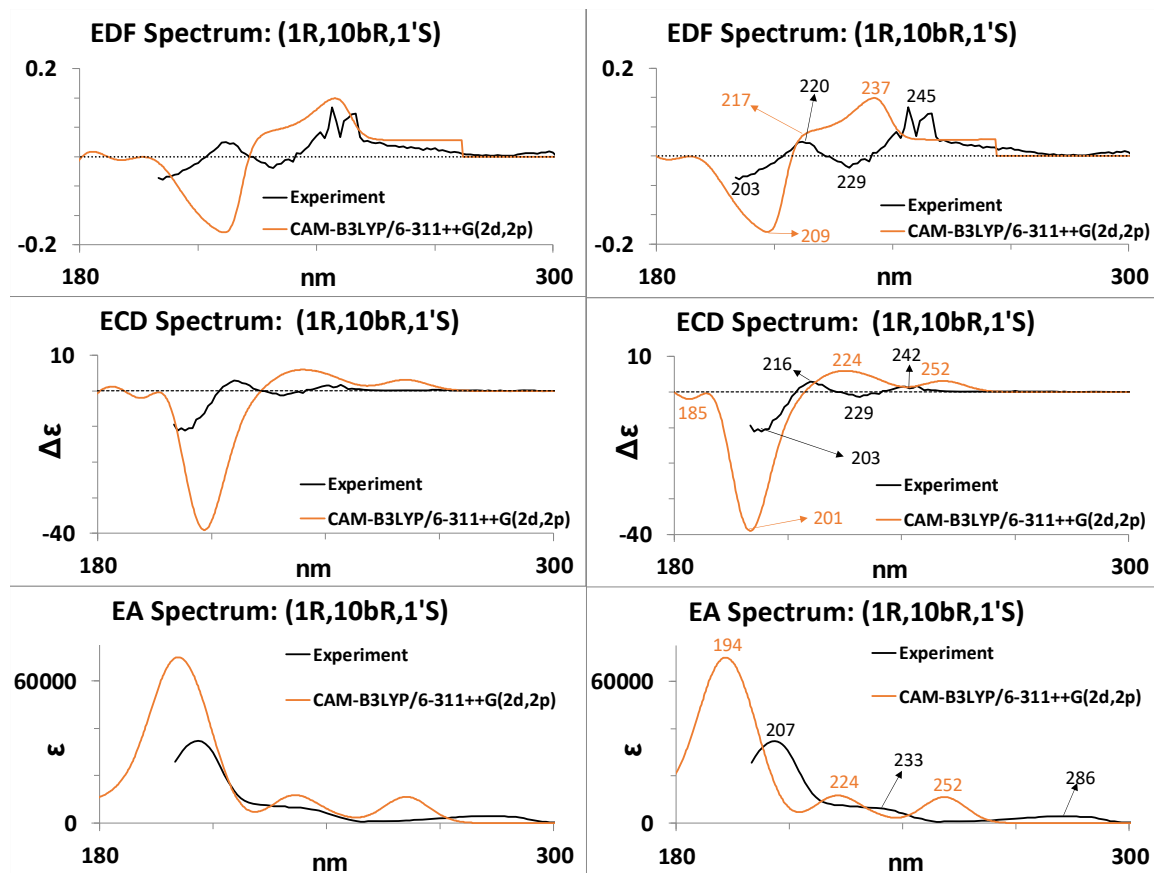


Figure S7. Comparison of experimental EA, ECD and EDF spectra of **5** with those predicted for (*1R,10bR,1'S*) diastereomer. The ECD spectra for (*1R,10bR,1'S*) diastereomer were obtained by multiplying the ECD of (*1S,10bS,1'R*) diastereomer with -1. In the left vertical panel, the predicted wavelengths are scaled with 1.04 (which corresponds to maximum SimECD value) and overlaid on experimental spectra. In the right vertical panel, QC predicted spectra obtained with unscaled band positions are presented.

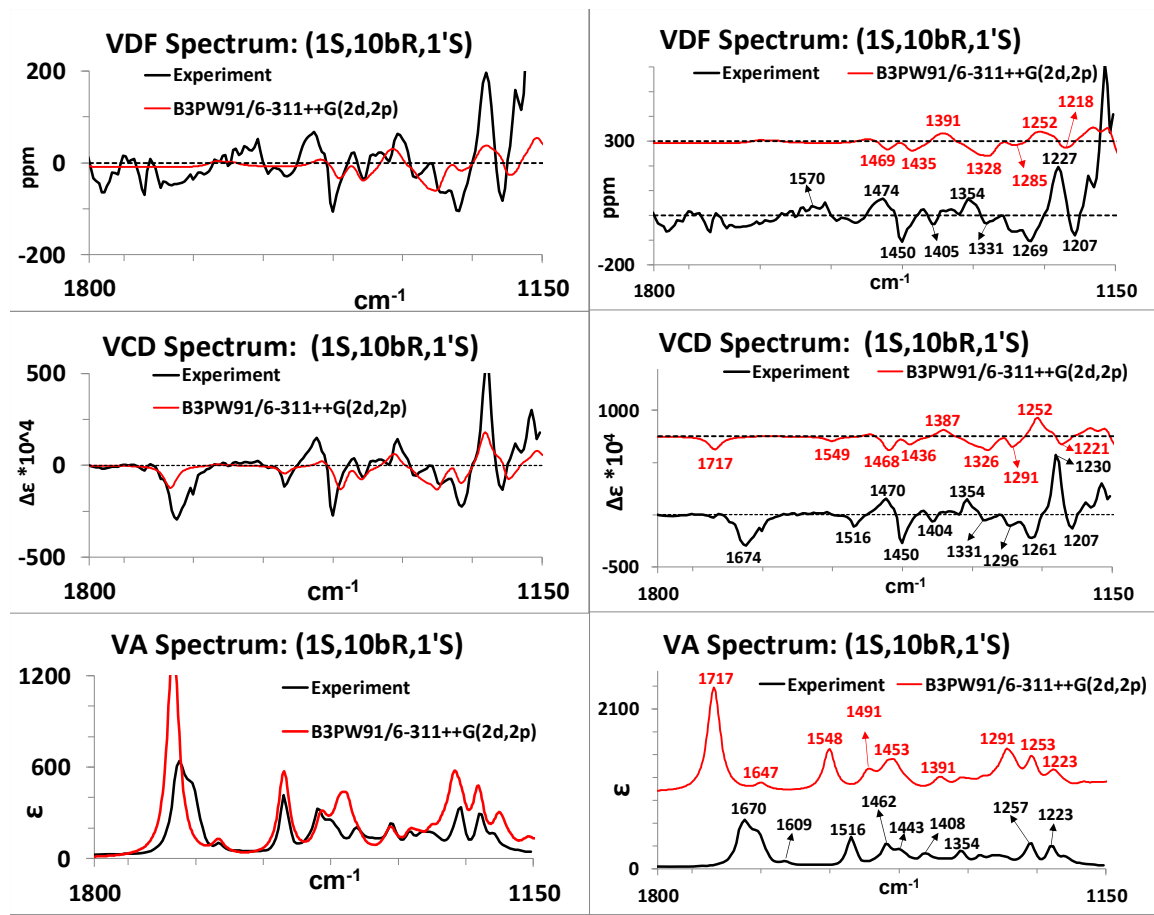


Figure S8. Comparison of experimental VA, VCD and VDF spectra of **5** with those predicted for (1S,10bR,1'S) diastereomer. The VCD spectra for (1S,10bR,1'S) diastereomer were obtained by multiplying the VCD of (1R,10bS,1'R) diastereomer with -1. In the left vertical panel, the predicted wavenumbers are scaled with 0.9795 (which corresponds to maximum SimVCD value) and overlaid on experimental spectra. In the right vertical panel, QC predicted spectra with unscaled wavenumbers are stacked over experimental spectra and band positions labeled.

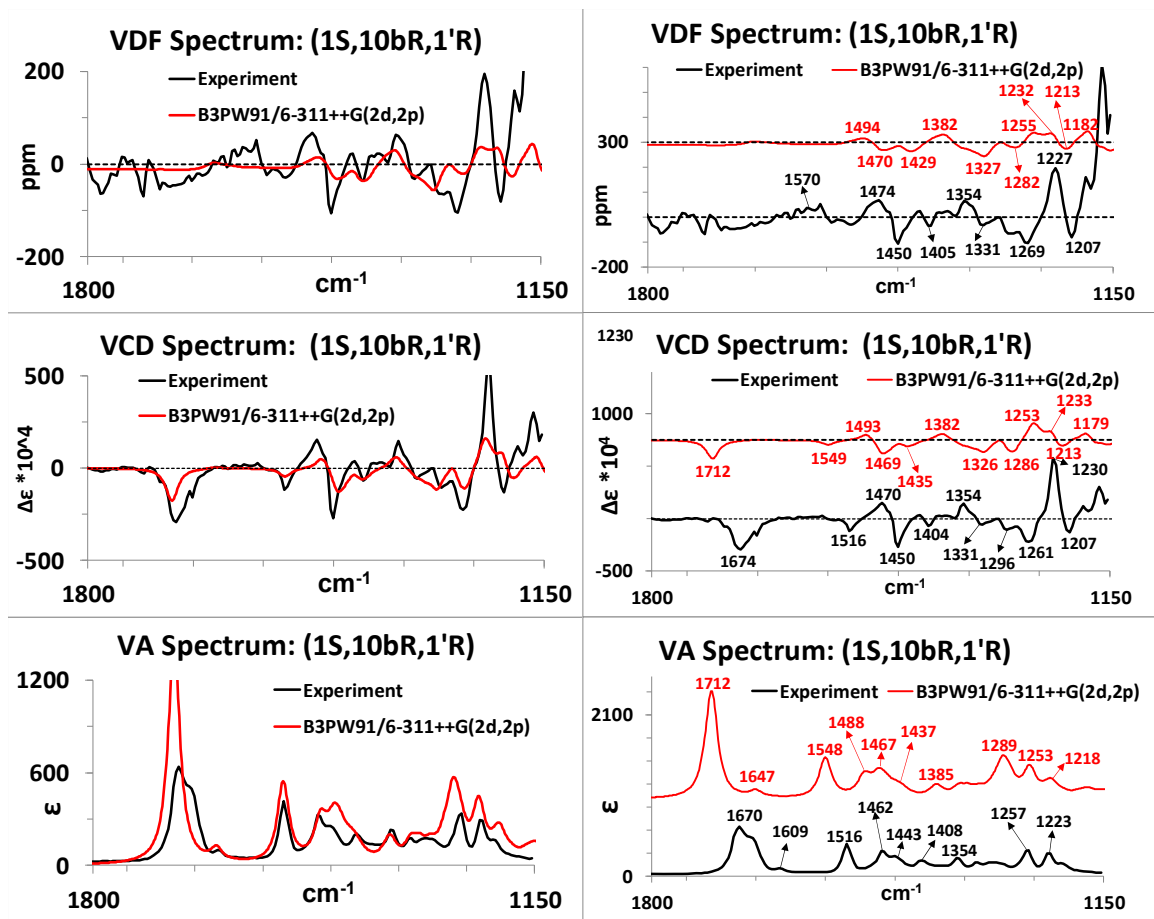


Figure S9. Comparison of experimental VA, VCD and VDF spectra of **5** with those predicted for (1S,10bR,1'R) diastereomer. In the left vertical panel, the predicted wavenumbers are scaled with 0.9805 (which corresponds to maximum SimVCD value) and overlaid on experimental spectra. In the right vertical panel, QC predicted spectra with unscaled wavenumbers are stacked over experimental spectra and band positions labeled.

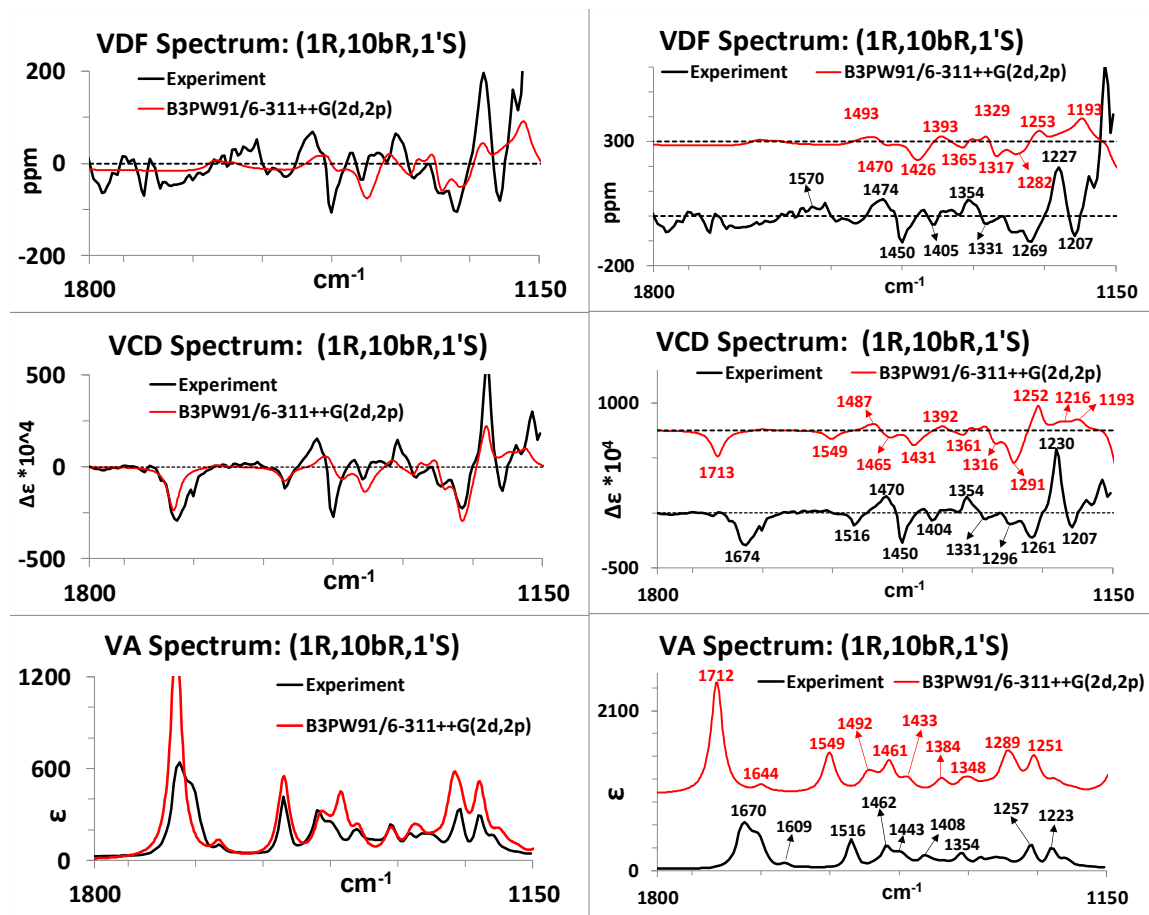


Figure S10. Comparison of experimental VA, VCD and VDF spectra of **5** with those predicted for (1*R*,10*bR*,1'*S*) diastereomer. The VCD spectra for (1*R*,10*bR*,1'*S*) diastereomer were obtained by multiplying the VCD of (1*S*,10*bS*,1'*R*) diastereomer with -1. In the left vertical panel, the predicted wavenumbers are scaled with 0.9795 (which corresponds to maximum SimVCD value) and overlaid on experimental spectra. In the right vertical panel, QC predicted spectra with unscaled wavenumbers are stacked over experimental spectra and band positions labeled.